

# Fire changes the spatial pattern and dynamics of soil nitrogen (N) and $\delta^{15}\text{N}$ at a grassland-shrubland ecotone



Guan Wang <sup>a,b</sup>, Junran Li <sup>a,\*</sup>, Sujith Ravi <sup>c</sup>, Bethany Theiling <sup>d</sup>, William Burger <sup>c</sup>

<sup>a</sup> Department of Geosciences, The University of Tulsa, Tulsa, OK, 74104, USA

<sup>b</sup> School of Soil and Water Conservation, Beijing Forestry University, Beijing, 100083, China

<sup>c</sup> Department of Earth and Environmental Science, Temple University, Philadelphia, PA, 19122, USA

<sup>d</sup> NASA Goddard Space Flight Center, Greenbelt, MD, 20771, USA

## ARTICLE INFO

### Keywords:

Soil nitrogen  
Fire-induced  
Microsite-scale  
Spatial pattern  
Grass-shrub competition

## ABSTRACT

Fire disturbance represents a major driver of soil nitrogen (N) distribution in many arid and semiarid grasslands. The spatial patterns of soil N and  $\delta^{15}\text{N}$  at microsite scale following fires, however, are rarely studied. Here we investigated the spatial distribution of soil N and soil  $\delta^{15}\text{N}$  before and within three years after a prescribed fire in a grassland-shrubland ecotone in the northern Chihuahuan Desert. The spatial heterogeneity of soil N decreased significantly after the fire, with the autocorrelation distance increasing from 1.55 m to over 3 m, and the spatial dependence index decreasing from 99% to 73%. Soil  $\delta^{15}\text{N}$  was autocorrelated at 0.44 m after the fire, a much smaller scale that is similar to recovered grass patches, suggesting grasses tend to control the soil N cycling rather than shrubs. Different from the overall content of soil N, which merely changed before and after fire, soil  $\delta^{15}\text{N}$  increased substantially after the fire. We argued that high temperature and increased soil moisture at grass microsites post-fire may lead to an enhanced mineralization rate and  $^{15}\text{N}$ -enriched soil ammonium at grass microsites, which further stimulates the rapid recovery of grasses after the fire.

## 1. Introduction

The transition of grassland to shrubland has dramatically altered land cover patterns in many arid and semiarid systems worldwide, resulting in substantial soil loss, decreased livestock production, and exacerbated desertification (Van Auken 2000; Puttock et al., 2014). As this vegetation transition process may take decades, some management tools may be used to mitigate or avert the shrub proliferation before it crosses an ecological threshold (Hoffmann et al., 2012). Recent work has demonstrated that periodic fire favors the homogenization of soil resources and can provide some form of reversibility for the grass-shrub transition in some grasslands (Ravi et al., 2009; White 2011; Wang et al., 2019). However, fire also leads to accelerated wind and water erosion, which may redistribute and deplete soil nutrients, causing permanent decline in soil quality (Austin et al., 2004; Ravi et al., 2012).

Soil nitrogen (N) is the most important essential macronutrient in desert ecosystems and is critical to plant establishment and survival, therefore its spatial distribution and enrichment affect the competition between grasses and shrubs substantially (Jarvie et al., 2012). Along

with the woody shrub encroachment process, nitrogen enriched soil tends to be eroded from the bare soil and then deposited in areas under the shrub canopies, resulting in enhanced soil heterogeneity, which further advances shrubs' competitive advantages against grasses (Ravi et al., 2009). It is generally recognized that the shrub proliferation lowers the availability of N in arid ecosystems and aggravates soil degradation (Li et al., 2008). Prescribed fire is considered as management option for restoring grasslands as well as for retarding the soil nutrients loss (Wang et al., 2018). Fire can influence soil N cycling through heating effects on soils, ash deposition of N that is previously contained in vegetation, relocation of soil water, alteration of soil microclimate by removal of vegetation/litter, and changes in microbial N mobilization (Grogan et al., 2000). However, the impact of fire on soil N cycling at microsite-scale, namely among individual plant sites and bare interspaces, is not well-documented. Such information is critically needed before the prescribed fire can be considered as an adaptive management approach.

Soil  $\delta^{15}\text{N}$  is a natural tracer of soil N cycling processes, which is often used to trace soil N cycling changes (Robinson 2001; Wang et al., 2013).

\* Corresponding author.

E-mail addresses: [guw647@utulsa.edu](mailto:guw647@utulsa.edu) (G. Wang), [junran-li@utulsa.edu](mailto:junran-li@utulsa.edu) (J. Li), [tuf77011@temple.edu](mailto:tuf77011@temple.edu) (S. Ravi), [bethany.p.theiling@nasa.gov](mailto:bethany.p.theiling@nasa.gov) (B. Theiling), [tud13441@temple.edu](mailto:tud13441@temple.edu) (W. Burger).

In dryland ecosystems, soil  $\delta^{15}\text{N}$  compositions are determined by the isotopic compositions of N inputs, fractionations related to N transformations, and N losses (Wang et al., 2013). Besides the original soil substrate, vegetation directly affects the soil  $\delta^{15}\text{N}$  value via litter decomposition and N assimilation (Lajtha and Schlesinger 1986). Soil water content also indirectly affects soil  $\delta^{15}\text{N}$  values because soil moisture dynamics strongly control soil N transformations (e.g., mineralization, nitrification, denitrification, and leaching) in arid environments (D'Odorico et al., 2003; Austin et al., 2004). Thus, the investigation of soil  $\delta^{15}\text{N}$  composition and variation may provide an alternative way to explore how soil N cycling responds to fires in grassland-shrubland transition zones without necessarily evaluating in detail all the processes involved in soil N cycling.

The objective of this study is to quantify the fine-scale spatial distribution and variations of soil N and  $\delta^{15}\text{N}$  as well as the subsequent ecosystem recovery after a prescribed fire at a grassland to shrubland transition system. Given the fact that fire has been frequently used as a management tool and N is the limiting nutrient in many arid and semiarid lands, the interactions between fire and soil N may provide implications for future land management under projected change in climate and fire regime.

## 2. Methods

### 2.1. Site description

The study site is located at the Sevilleta National Wildlife Refuge

(SNWR) in the northern Chihuahuan Desert, New Mexico, United States (Fig. 1a). The SNWR is the primary study site of the Sevilleta Long Term Ecological Research (LTER) project. At the SNWR, the northward invasion of woody shrubs, such as creosotebush (*L. tridentata*) and mesquite (*Prosopis glandulosa* Torr.) into perennial grasslands has been well documented, primarily due to cattle grazing, climatic changes and fire suppression (Báez and Collins 2008; Van Auken 2009; Sankey et al., 2012; Puttock et al., 2014). This site is dominated by black grama (*Bouteloua eriopoda*) and the encroachment of woody shrubs is at the moderate level (Sankey et al., 2012; Cunliffe et al., 2016). The soil texture is primarily sandy loam (Cunliffe et al., 2016).

The land surface comprises 60% grass coverage, 5–10% shrub coverage, and 30%–35% bare soil (Fig. 1b, Dukes et al., 2018). The vegetation connectivity is sufficient for fires to spread under strong winds (ideally 5 m/s or higher) (Ravi et al., 2009). The windy season is from March to May and the predominant wind is from the southwest. Annual precipitation is 250 mm and most precipitation occurs from June to September (Báez and Collins 2008). The landscape is composed of three types of microsite, namely grass microsite, shrub microsite, and bare interspace microsite, representing areas with grass cover, under shrub canopies, and with bare soil, respectively. The diameter of a single microsite patch is usually < 1 m for grass microsites, and 1 m–2 m for shrub microsites. Bare interspaces are the unvegetated areas between vegetated patches with varied size (Fig. 1e).

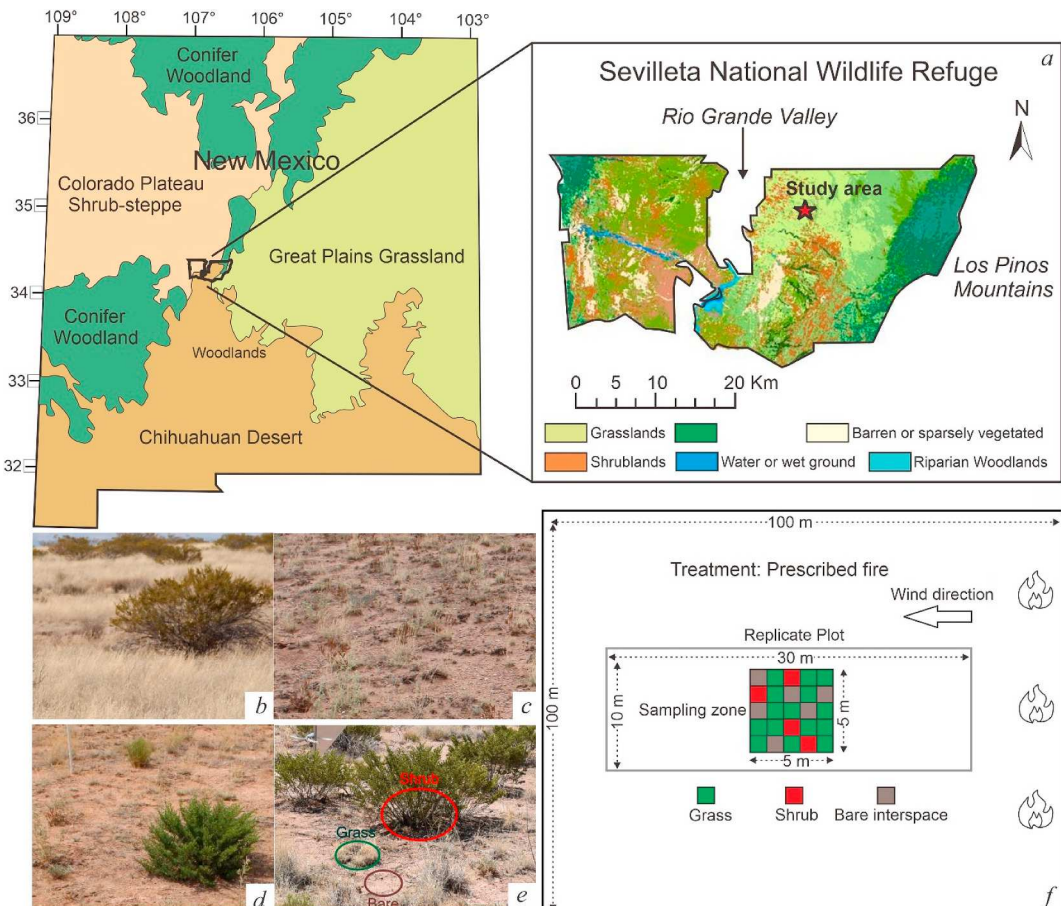


**Fig. 1.** (a) Location of the study area in the Sevilleta National Wildlife Refuge (SNWR) in the northern Chihuahuan Desert, New Mexico, USA; (b) The surface condition of the study area in Mar. 2016 before the prescribed fire; (c) Jun. 2016 after one windy season; (d) Jun. 2017 after two windy seasons; (e) Jun. 2018 after three windy seasons; and (f) Experimental setup and sampling in the field, which consists of three replicate plots (30 × 10 m) each containing a sampling zone (5 × 5 m). The brown, green and red circles show the land surface characteristics of bare, grass, and shrub microsites, respectively.

## 2.2. Field experiments

In March 2016, a 100 m × 100 m monitoring area was established in the study area (Fig. 1f). A prescribed fire was set to burn the monitoring area on March 10, 2016, before the beginning of the spring windy season. The fire was ignited using hydrocarbons on the windward edge of the area and was confined within the monitoring area. The vegetation cover provided enough connectivity among plant patches for the fire to propagate. Partially burnt shrubs were subsequently torched to ensure the complete removal of aboveground vegetation. The monitoring area consists of three 30 m × 10 m replicated plots. The plots are oriented with the short-axis perpendicular to the predominant wind direction to minimize interactions. In the middle of each 30 m × 10 m plot, a 5 m × 5 m sampling area was established for soil samples collection. The locations for each corner of these rectangle plots and sampling areas were labeled by a hand-held differential GPS receiver for reference.

Within each (5 m × 5 m) sampling plot, 50 randomly distributed soil samples were collected with a spade from surface soil (top 3 cm) one day before the prescribed fire and after every year's spring windy season during the following three years. The coordinates of the sampling locations were randomly generated in R software (R Core Team, 2017), and a different set of sampling locations was used for each sampling period. During the process of soil sampling, locations of the soil samples were carefully determined using a centimeter-scale coordinate system based on the 5 m × 5 m sampling area (Fig. 1f). The microsite type of every sampling point was also manually recorded.

Vegetation foliar samples, including every visible species in the study area, were randomly collected from the monitoring area and the nearby unburned area in September 2017. Species name, locations (from burned, unburned areas), and vegetation types of the foliar samples were recorded. Plant cover and community composition of the treated area were monitored by four 50-m line intercept transects (parallel and perpendicular to wind direction) a day before the fire and in every June from 2016 to 2018. The plant canopy height and width, as well as the bare interspace width were measured along transects.

In the laboratory, each soil sample was passed through a 2-mm sieve to remove roots, coarse surface litter, and rock fragments (pebbles, gravels, cobbles). Plant debris was also carefully removed by hand from the soil samples. Soil samples were then air-dried and ground to fine powder by a ball mill (PBM-04 Planetary Ball Mill, RETSCH, Germany). Vegetation samples were first rinsed with deionized water to remove the attached dust and ashes, and then oven-dried at 60 °C for 48 h. The vegetation samples were then ground into small pieces using a mortar and pestle. The soil samples were then removed to 5 × 9 mm tin capsules.  $\delta^{15}\text{N}$  and TN in soil and vegetation samples were measured via flash combustion and reduction using a Thermo Finnigan Flash HT EA (high temperature elemental analyzer) coupled to a Thermo Finnigan Conflo IV and Thermo Finnigan Delta V Advantage isotope ratio mass spectrometer (IRMS).

Nitrogen stable isotope compositions are reported in the conventional form:

$$\delta^{15}\text{N}(\text{\textperthousand}) = \left[ \left( ^{15}\text{N}/^{14}\text{N} \right)_{\text{sample}} / \left( ^{15}\text{N}/^{14}\text{N} \right)_{\text{AIR}} - 1 \right] \times 1000$$

where  $(^{15}\text{N}/^{14}\text{N})_{\text{sample}}$  and  $(^{15}\text{N}/^{14}\text{N})_{\text{AIR}}$  are the isotopic ratios of the sample and international reference for atmospheric  $\text{N}_2$  (AIR), respectively. Precision of triplicate measurements for sample  $\delta^{15}\text{N}$  is 0.1‰. Reproducibility and calibration of TN and  $\delta^{15}\text{N}$  measurements are determined during each batch of samples by replicate measurements of two internal standards (acetanilide and sulfanilamide), plus the national standard USGS 40 (L-glutamic acid). Precision for standards is  $\leq 0.1\text{\textperthousand}$ .

## 2.3. Data analysis

For each sampling period, we calculated the mean values of  $\delta^{15}\text{N}$  and TN for the entire sampling area as well as samples from different

microsites. The coefficient of variations of  $\delta^{15}\text{N}$  and TN were also calculated to evaluate the overall variations among samples. The distribution of TN and  $\delta^{15}\text{N}$  were tested for normality by Shapiro-Wilk normality test in R (R Core Team, 2017). The variance for TN and  $\delta^{15}\text{N}$  along different periods were tested by Levene's Test through car package in R (Fox and Weisberg, 2019). For all values not passing the normality test, we used a natural logarithmic transformation prior to analysis. One-way ANOVA was conducted to compare the mean values of  $\delta^{15}\text{N}$  and TN in different sampling periods. The significance of difference for the coefficient of variation (CV) of TN and soil  $\delta^{15}\text{N}$  among different sampling periods was tested by Feltz and Miller's asymptotic test (1996) and cross-validated with Krishnamoorthy and Lee's modified signed-likelihood ratio test (2014). Two-way ANOVA was conducted to identify the difference of  $\delta^{15}\text{N}$  and TN among different microsites (factor 1), and among different sampling periods (factor 2). Significance of differences between two specific means were assessed with a post hoc Tukey HSD test. For the three most common plants in the study area, the foliar TN and  $\delta^{15}\text{N}$  contents of samples from burned and unburned areas were compared using *t*-Test. Unless otherwise indicated, we set  $P < 0.05$  for significance. The above data analyses were performed using R software (R Development Core Team, 2017; Marwick and Krishnamoorthy, 2019).

The characteristics of the spatial distribution of soil  $\delta^{15}\text{N}$  and TN were quantified using geostatistical analyses. Semivariograms, which depict the average variance found in comparisons of samples taken at increasing distance from one another (Schlesinger et al., 1996), were performed for soil  $\delta^{15}\text{N}$  and TN of each sampling period. A semivariogram was created using the lag interval of 0.2 m in each 5 m × 5 m sampling plot. When comparing the isotropic and corresponding anisotropic semivariograms at 0°, 45°, 90° and 135°, no significant directional patterns was found. Therefore, isotropic semivariograms were used in all analyses in this study. The spherical model was used to fit the empirical soil  $\delta^{15}\text{N}$  and TN distribution (Schlesinger et al., 1996; Li et al., 2008), and three important parameters were obtained, namely,  $A_0$  (range),  $C_0$  (nugget variance), and  $C$  (structural variance). The formula of the spherical model is:

$$\gamma(h) = C_0 + \frac{1}{2} C \left[ \frac{3h}{A_0} - \frac{h^3}{A_0^3} \right] \quad h < A_0$$

$$\gamma(h) = C_0 + C \quad h > A_0$$

where  $h$  is the lag interval,  $A_0$  is the range,  $C_0$  is the nugget variance, and  $C$  is the structural variance. Range ( $A_0$ ) represents the distance of spatial autocorrelation.  $C/(C_0+C)$  indicates the magnitude of spatial dependence. A high  $C/(C_0+C)$  ratio suggests a strong spatial pattern, whereas a low ratio implies a random pattern (Schlesinger et al., 1996). The geostatistical analyses were conducted using the GS + package (GS + version 10, Gamma Design Software, Plainwell, Michigan).

## 3. Results

### 3.1. Change of soil $\delta^{15}\text{N}$ , and TN

Overall, fire did not change the average soil TN content significantly during the experimental period ( $P = 0.12$ , ANOVA). The soil  $\delta^{15}\text{N}$  composition, however, increased from +5.3‰ before the fire to +5.6‰ three seasons after the fire ( $P < 0.05$ , ANOVA) (Table 1). The coefficient of variation (CV) of both TN and  $\delta^{15}\text{N}$  decreased substantially following the fire (Table 1). The post-fire recovery of grasses was notably faster than shrubs, and by June 2018, nearly 70% of the grass cover was recovered in the study area.

The changes of soil TN and  $\delta^{15}\text{N}$  among different microsites are shown in Fig. 2. Shrub microsites had significantly higher and more variable TN than grass and bare microsites prior to and immediately following the fire, but this significant difference disappeared in June

**Table 1**

Mean value ( $\pm$ standard error) and coefficient of variation (CV) of soil total nitrogen (TN) and soil  $\delta^{15}\text{N}$  (‰), and fractional vegetation cover (plant cover %) in the study area during the experimental period.

Time period	TN		$\delta^{15}\text{N}$		Plant cover (%)	
	Mean (mg/g)	CV (%)	Mean (‰)	CV (%)	Shrub	Grass
Pre-burn	0.82 <sup>a</sup> $\pm$ 0.046	40.2 <sup>a</sup>	5.3 <sup>a</sup> $\pm$ 0.189	25.5 <sup>a</sup>	17	47
June 2016	0.83 <sup>a</sup> $\pm$ 0.045	38.3 <sup>a</sup>	5.8 <sup>b</sup> $\pm$ 0.114	14.0 <sup>b</sup>	1	18
June 2017	0.75 <sup>a</sup> $\pm$ 0.032	30.3 <sup>b</sup>	5.7 <sup>b</sup> $\pm$ 0.125	15.5 <sup>b</sup>	4	22
June 2018	0.88 <sup>a</sup> $\pm$ 0.025	21.5 <sup>b</sup>	5.6 <sup>b</sup> $\pm$ 0.111	14.4 <sup>b</sup>	5	33

Note: letters indicate significant difference for TN and soil  $\delta^{15}\text{N}$  between two sampling times (One way ANOVA,  $P < 0.05$ ), and significant difference for CV of TN and soil  $\delta^{15}\text{N}$  between two sampling times (Feltz and Miller's (1996) asymptotic test and cross-validated with Krishnamoorthy and Lee's (2014) modified signed-likelihood ratio test,  $P < 0.05$ ).

2017 (Fig. 2a). For TN, the two-way ANOVA results exhibited significant differences for both period ( $P < 0.001$ ) and microsite type ( $P < 0.001$ ) (Supplementary Table 1). For soil  $\delta^{15}\text{N}$ , bare and grass microsites generally had the highest and lowest values, respectively among the three types of microsites during the experimental period (Fig. 2b). The two-way ANOVA results for soil  $\delta^{15}\text{N}$  revealed significance differences existed for microsite types ( $P < 0.001$ ) but not periods ( $P > 0.05$ ), while the interaction between period and microsite types is also significant ( $P < 0.01$ ) (Supplementary Table 2).

Geostatistical analyses further revealed the spatial distribution patterns of soil TN and  $\delta^{15}\text{N}$  (Fig. 3). Before the prescribed fire, soil TN was autocorrelated over a distance of 1.55 m, and this distance varied in the subsequent sampling periods and reached 3.24 m in June 2018. The distance of autocorrelation for soil  $\delta^{15}\text{N}$  is generally smaller than that of soil TN for a given sampling period, but no consistent pattern was found during the experimental period. The spatial dependence index, representing the strength of the spatial structure, decreased continuously for TN (from 99% to 73%), but stayed >95% for soil  $\delta^{15}\text{N}$  in all sampling periods.

### 3.2. Vegetation $\delta^{15}\text{N}$

The foliar N and  $\delta^{15}\text{N}$  contents of creosote bush are 2.63% and 7.5‰ respectively, which are substantially higher than those of black gramma (0.74% and 4.3‰) and sand muhly (1.28% and 3.3‰), regardless of the fire (Table 2). In contrast to the foliar N content, which merely changed after fire, the  $\delta^{15}\text{N}$  of herbaceous plants in burned area (4.3‰) was lower than in nearby unburned areas (4.5‰), while for creosote bush, the  $\delta^{15}\text{N}$  in burned area (7.5‰) was higher when comparing to the same plant in nearby unburned areas (6.9‰) (Table 2).

## 4. Discussion

Spatial patterns of soil TN and  $\delta^{15}\text{N}$  provide integrative insights on change of soil N pools when disturbance occurred (Rascher et al., 2012; Zhou et al., 2018). The high TN and soil  $\delta^{15}\text{N}$  concentrations at the shrub microsites prior to fire are consistent with the high N content and high  $\delta^{15}\text{N}$  of shrub leaves when comparing to grasses, suggesting that the majority of shrub litters are localized under the shrub canopies, which is congruent with a well-documented phenomenon: the formation of islands of fertility, initiated when the shrub canopies modify the surface roughness, micro-climate and micro-topography in a landscape, resulting in accumulation of nutrients under shrubs and depleting of nutrients in grass and unvegetated areas (Schlesinger et al., 1996; Field et al., 2012; Puttock et al., 2013, Gonzales et al., 2018). Nutrients that were previously immobilized in biomass are deposited as ash after the fire, which leads to increased pH and enhanced base saturation of the topsoil layer (Butler et al. 2018), further increasing the denitrification and denitrification after fire. Wang et al. (2018) indicated that soil water content is highest in shrub microsites and low in grass and bare microsites without fire. The highest soil  $\delta^{15}\text{N}$  at the bare interspaces suggests that bare soil may be “hotspots” of high denitrification, and volatilization, due to relative high temperature, low litter input, low soil water content, and high run-off during rain events. The process of N leaching at the bare interspaces, although not quantified in this study, is likely to decrease as the nitrate would be consumed in denitrification.

The high CV and high magnitude of spatial dependence for TN and  $\delta^{15}\text{N}$  indicate a heterogeneous soil N distribution at the microsite-scale

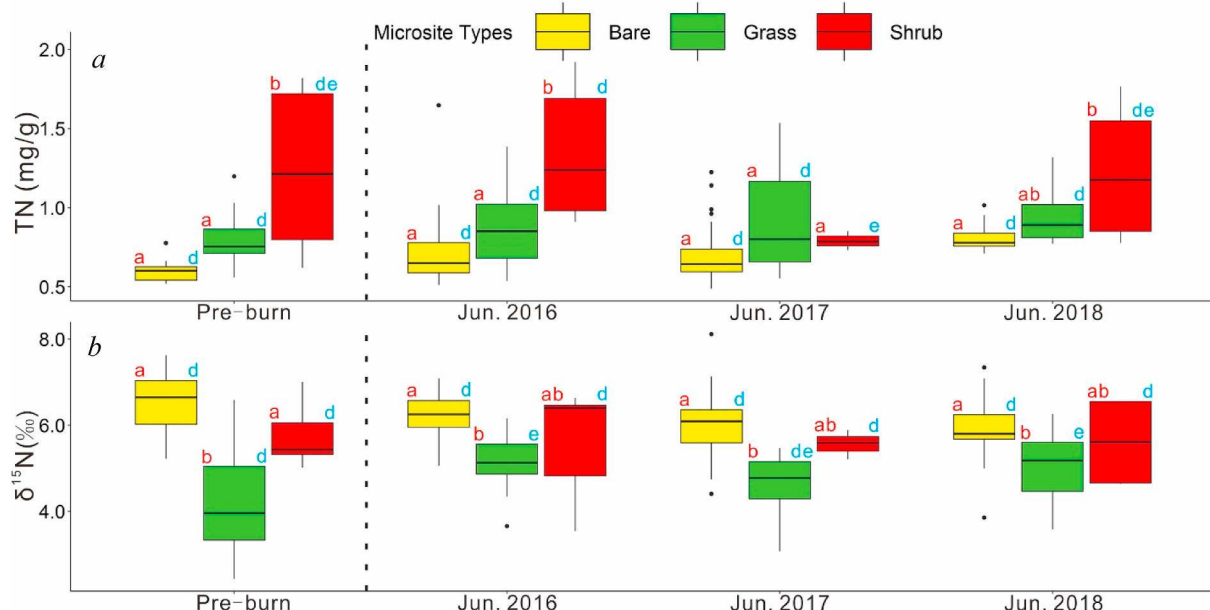


**Fig. 2.** The change of TN (a) and soil  $\delta^{15}\text{N}$  composition (b) at different microsites during the experimental period. A two-way ANOVA was conducted for the treated area. The red letters (on the left side of each box) show the statistical results for different microsites at each sampling time, and the blue letters (on the right side of each box) indicate the results for the same microsite at different sampling times. Significance of difference is exhibited by different letters ( $P < 0.05$ ). Dashed line indicates before and after the prescribed fire. Note the horizontal bars in the boxes are medians.

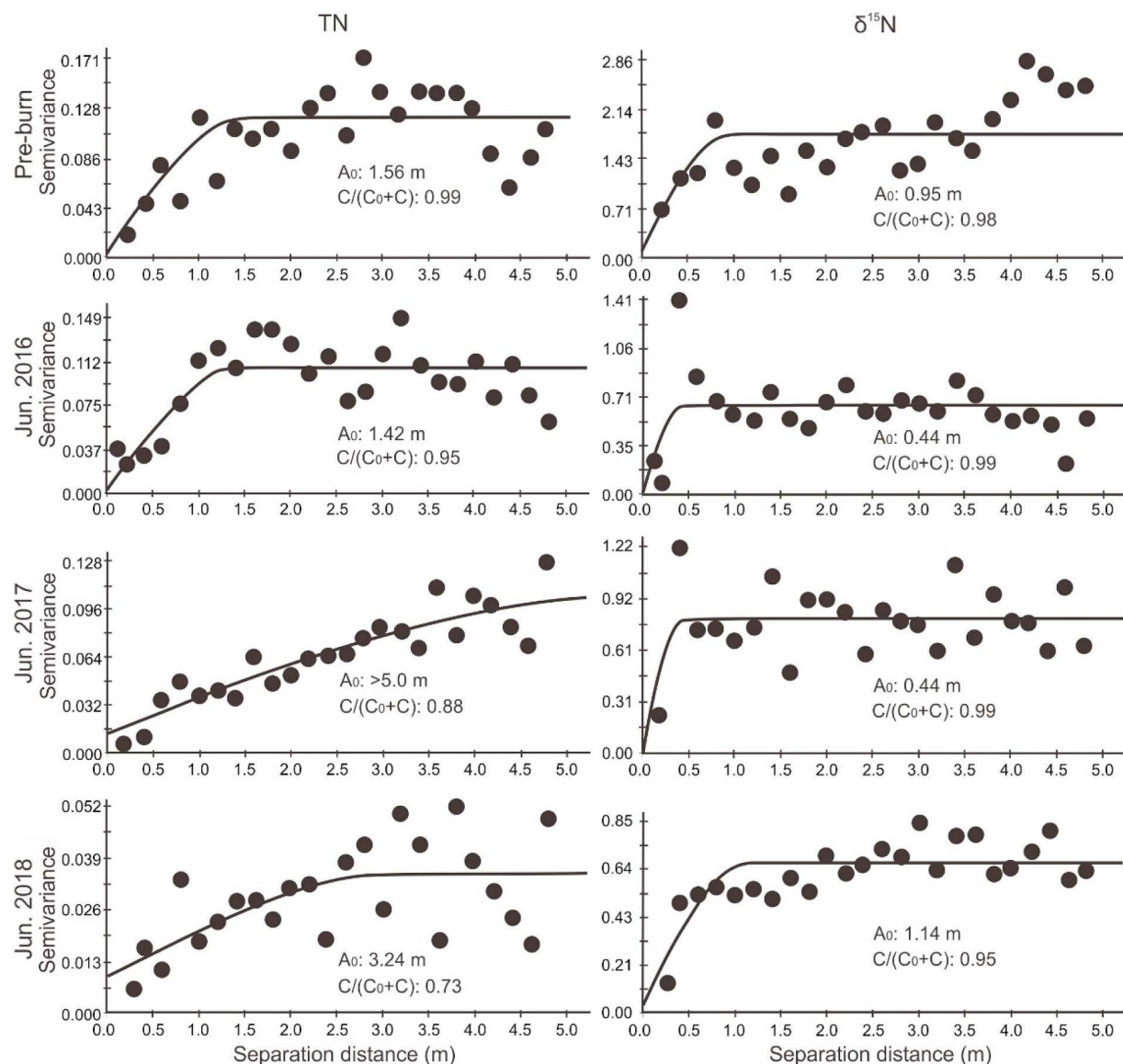


**Fig. 3.** Semivariograms of soil TN and  $\delta^{15}\text{N}$  distribution before and after the prescribed fire during the experimental period. Under the curve is the summary of semivariogram spherical model parameters.  $A_0$  is the spatial autocorrelation distance, and  $C/(C_0 + C)$  represents the ratio of structured variance among the samples.

**Table 2**  
Foliar TN and  $\delta^{15}\text{N}$  content for the three most common plants in the study area.

Plant types	Plant species	N (%)		$\delta^{15}\text{N}$ (%)	
		Unburned	Burned recovery	Unburned	Burned recovery
Grass	Black grama	0.74 <sup>a</sup>	0.77 <sup>a</sup>	4.5 <sup>a</sup>	4.3 <sup>b</sup>
Shrub	Sand muhly	1.18 <sup>a</sup>	1.28 <sup>b</sup>	4.8 <sup>a</sup>	3.3 <sup>b</sup>
Shrub	Creosote bush	2.63 <sup>a</sup>	2.63 <sup>a</sup>	6.9 <sup>a</sup>	7.5 <sup>b</sup>

Note: letters indicate significant difference for foliar TN and  $\delta^{15}\text{N}$  for each plant species in burned and unburned areas (*t*-test,  $P < 0.05$ ).

before the fire. Most of the soil organic matter inputs occur in the form of litter for shrubs (thus staying in the top 3 cm), while grass tends to have a dense network of fine roots so that soil organic matter inputs for grass occur below the 3 cm depth. The spatial autocorrelation distance (1.55 m) of soil TN displayed a strong resemblance to the common shrub canopy size (1–2 m), suggesting that the distribution of soil N is mainly

controlled by shrubs, which also appeared in other grass-shrub coexisting systems in the Chihuahua Desert (e.g., Li et al., 2008). The highest TN content in shrub microsites further confirmed shrub's ability for N accumulation. Unlike soil TN, the much smaller (0.95 m) spatial autocorrelation distance of soil  $\delta^{15}\text{N}$  was observed before fire. This suggests that the  $\delta^{15}\text{N}$  values of foliar organic N inputs is not the sole determinant of soil  $\delta^{15}\text{N}$  in this grassland-shrubland transition zone, and other biotic or abiotic factors also affect the soil N fractionation. Different litter input and the related microbial activities in the soil surface beneath, on the edge, and outside of plant canopies may be one of the reasons (Throop et al., 2013). In addition, we observed that the boundaries for long-lived mature shrubs and grasses are sometimes obscure in the field, with grasses extending beneath shrub canopies, which may also contribute to the smaller spatial autocorrelation distance of soil  $\delta^{15}\text{N}$ .

Multiple observations suggest a more homogeneous distribution of N in the landscape after the fire. Examples are that the spatial autocorrelation distance of TN changed to >5.0 m, well beyond the shrub canopy diameter, the CV of TN decreased, and the significant difference of soil TN among grass, shrub, and bare microsite disappeared in June 2017. Such a change in soil N distribution is likely caused by enhanced wind

erosion and the altered source to sink pathways after the fire (Dukes et al., 2018). The atmospheric N deposition rate is low in the Northern Chihuahuan Desert (Baez et al., 2007), which merely affects the fine-scale distribution of TN. Previous studies demonstrated that, along with the woody plants encroachment, shrubs altered the microclimate for areas under the shrub canopies, creating high soil water content (SWC) and favorable soil temperature, making shrubs more competitive when competing with grasses (Throop et al., 2012; Wang et al., 2018). However, these competitive advantages of shrubs subdued after the fire, represented by the lowest soil water content (Wang et al., 2018) and higher daytime soil temperature of shrub microsites (Burger, 2019).

It is noteworthy that grass recovered more rapidly in the first two years following the fire (Table 1). During the windy seasons, newly germinated grasses and fibrous meristems of burned grasses captured  $\delta^{15}\text{N}$  enriched litters and wind-blown ashes, making soil  $\delta^{15}\text{N}$  concentrated in a scale similar to grass patches (0.44 m autocorrelation distance), which is in agreement with Ravi et al. (2009), illustrating that the grass rings in SNWR are approximately 30–60 cm in diameter. The increased litter input tended to increase the soil organic matter pool in grass microsites, which, in combination with high soil water content (Wang et al., 2018), lead to a higher mineralization rate, creating more soil ammonium that stimulated the following grass recovery. Besides, soil water content was very responsive to rain events at the microsite-scale, and the shrub microsites exhibited the lowest soil water content during the experimental period, while the bare and grass microsites had highest soil water content regardless of rains (Wang et al., 2018), which also contributed to the faster recovery of grasses.

The increased foliar  $\delta^{15}\text{N}$  of creosote bush is likely caused by the absorption of N from deep soil, which has higher  $\delta^{15}\text{N}$  than surface soil (Högberg 1997; Zhou et al., 2018). Despite the kill of the aboveground shrub biomass, the shrub roots below-ground may survive after the fire, which could extend to beyond 1 m (McCulley et al., 2004). Therefore, the re-sprouted shrubs utilize  $^{15}\text{N}$ -enriched ammonium or nitrates from deep soil, making new plants enriched in  $^{15}\text{N}$  (Cook 2001; Drewa et al., 2002). Different from deep-rooted shrubs, grasses in the study area are shallow-rooted, and the recovery of grasses mostly depends on the germination from seed (Grogan et al., 2000; Peters 2002), which absorbed from areas near surface soil with relatively lower  $\delta^{15}\text{N}$ . The increased SOC (soil organic carbon) from ashes makes N-fixing bacteria more active when fixing N from the atmosphere (Grogan et al., 2000; Ball et al., 2010), which added  $^{15}\text{N}$ -depleted ammonium to surface soil, acting as N sources for grasses, leading to decreased grass foliar  $\delta^{15}\text{N}$ .

The different change patterns for soil TN and  $\delta^{15}\text{N}$  suggest an altered decomposition process as well as N sources for different types of microsite. This is likely caused by the soil heating, ashes and incompletely burned organic matter, and volatilization. For bare microsites, their pre-fire N input is mainly determined by the abiotic processes due to the lack of vegetation cover, and these processes may be strongly affected by the seasonal changes of temperature, wind, precipitation etc. However, after fire, because of the redistribution of soil water and soil organic matter (Dukes et al., 2018; Wang et al., 2019), bare interspaces showed similar soil water content as grass microsites and received more plant litters, which may explain the similar N decomposition processes shared by grass and bare microsites.

Our results provide clues to illustrate the variation and possible changes of N content in a grassland-shrubland transition zone affected by fire. Before the fire, litter inputs lowered soil  $\delta^{15}\text{N}$  while decomposition increased soil  $\delta^{15}\text{N}$  (Craine et al., 2015). Areas at grass or shrub microsites generally have lower soil  $\delta^{15}\text{N}$  values than bare interspaces. Low grass foliar  $\delta^{15}\text{N}$  and high shrub foliar  $\delta^{15}\text{N}$ , which are the main soil nitrogen input to these microsites, further discriminate the soil  $\delta^{15}\text{N}$  between grass and shrub microsites. During a fire event, the consumption of litter on soil surface and volatilization of N lead to enriched soil  $\delta^{15}\text{N}$ , creating a boost of nitrogen back to the atmosphere (Levine et al., 1996). Increased soil  $\delta^{15}\text{N}$  was largely attributed by enhanced ammonification, creating enhanced ammonium in the soil (Augustine et al.,

2014). After the fire, N in the ash left on the surface typically tends to mineralize rapidly, because nutrients bound in dead plant tissues are converted into more available forms by fire (Qian et al., 2009). As a result, the microbial activities become highly active, leading to an accelerated N fixation from air and enhanced decomposition of soil organic matter (Callaway and Maron 2006). The rapid recovery of grasses and shrubs absorb N from shallow or deep soil, creating high assimilation rate. Meanwhile, N in surface soil may also increase slightly when litter-fall occurs (McClaran et al., 2008; Throop and Archer 2008).

Overall, our study shows the microsite-scale changes of the spatial distribution of soil N and  $\delta^{15}\text{N}$  affected by a prescribed fire at a shrub encroached grassland over a period of three years. Such changes highlight the function of fire on altering the spatial distribution of soil N as well as the exchanges among soil N cycling. The input of ashes, increased soil water content, and reduced spatial heterogeneity of soil nitrogen stimulated the rapid recovery of grasses, which strongly favor the grasses over shrubs in this grass-shrub coexisting system.

## CRediT authorship contribution statement

**Guan Wang:** Data curation, Formal analysis, Field work, laboratory analysis, data processing and analysis, manuscript, Writing - original draft, Writing - review & editing. **Junran Li:** Conceptualization, Funding acquisition, Supervision, Methodology, Project administration, Writing - review & editing. **Sujith Ravi:** Conceptualization, Funding acquisition, Methodology, Project administration, Writing - review & editing. **Bethany Theiling:** Formal analysis, Writing - review & editing, Data curation, Writing - review & editing.

## Declaration of competing interest

The authors declare that they have no known competing financial interests or personal relationships that could have appeared to influence the work reported in this paper.

## Acknowledgement

This research was supported by the U.S. National Science Foundation (NSF) Award EAR-1451489 and NASA grant 80NSSC19K0195 for J. Li, NSF EAR-1451518 for S. Ravi, and the Sevilleta LTER Summer Research Fellowship for G. Wang. The authors greatly acknowledge Scott Collins, Stephanie Baker, and Amaris Swan (Sevilleta LTER, New Mexico), Jon Erz, Eric Krueger and Andy Lopez (FWS, SNWR), and Julie McDonald and Bradley Claggett (The University of Tulsa) for their assistance in field work and laboratory analysis.

## Appendix A. Supplementary data

Supplementary data to this article can be found online at <https://doi.org/10.1016/j.jaridenv.2020.104422>.

## References

- Austin, A.T., Yahdjian, L., Stark, J.M., Belnap, J., Porporato, A., Norton, U., Ravetta, D.A., Schaeffer, S.M., 2004. Water pulses and biogeochemical cycles in arid and semiarid ecosystems. *Oecologia* 141, 221–235. <https://doi.org/10.1007/s00442-004-1519-1>.
- Baez, S., Collins, S.L., 2008. Shrub invasion decreases diversity and alters community stability in northern Chihuahuan Desert plant communities. *PLoS One* 3, e2332. <https://doi.org/10.1371/journal.pone.0002332>.
- Ball, P.N., MacKenzie, M.D., DeLuca, T.H., Montana, W.E., 2010. Wildfire and charcoal enhance nitrification and ammonium-oxidizing bacterial abundance in dry montane forest soils. *J. Environ. Qual.* 39, 1243–1253. <https://doi.org/10.2134/jeq2009.0082>.
- Burger, W., 2019. In: *Spatial Analysis of Post-fire Sediment Redistribution Using Rare Earth Element Tracers*. Temple University. MS Thesis.
- Callaway, R.M., Maron, J.L., 2006. What have exotic plant invasions taught us over the past 20 years? *Trends Ecol. Evol.* 21, 369–374. <https://doi.org/10.1016/j.tree.2006.04.008>.

Cook, G.D., 2001. Effects of frequent fires and grazing on stable nitrogen isotope ratios of vegetation in northern Australia. *Austral Ecol.* 26, 630–636. <https://doi.org/10.1046/j.1442-9993.2001.01150.x>.

Craine, J.M., Brookshire, E.N.J., Cramer, M.D., Hasselquist, N.J., Koba, K., Marin-Spiotta, E., Wang, L., 2015. Ecological interpretations of nitrogen isotope ratios of terrestrial plants and soils. *Plant Soil* 396, 1–26. <https://doi.org/10.1007/s11104-015-2542-1>.

Cunliffe, A.M., Puttock, A.K., Turnbull, L., Wainwright, J., Brazier, R.E., 2016. Dryland, calcareous soils store (and lose) significant quantities of near-surface organic carbon. *J. Geophys. Res.: Earth Surface* 121, 684–702. <https://doi.org/10.1002/2015JF003628>.

Drewa, P.B., Platt, W.J., Moser, E.B., 2002. Fire effects on resprouting of shrubs in headwaters of southeastern longleaf pine savannas. *Ecology* 83, 755–767.

Dukes, D., Gonzales, H.B., Ravi, S., Grandstaff, D.E., Van Pelt, R.S., Li, J., Wang, G., Sankey, J., 2018. Quantifying postfire aeolian sediment transport using rare earth element tracers. *J. Geophys. Res.: Biogeosciences* 123, 288–299. <https://doi.org/10.1002/2017JG004284>.

D'Odorico, P., Laio, F., Porporato, A., Rodriguez-Iturbe, I., 2003. Hydrologic controls on soil carbon and nitrogen cycles. II. A case study. *Adv. Water Resour.* 26, 59–70. [https://doi.org/10.1016/S0309-1708\(02\)00095-7](https://doi.org/10.1016/S0309-1708(02)00095-7).

Field, J.P., Breshears, D.D., Whicker, J.J., Zou, C.B., 2012. Sediment capture by vegetation patches: implications for desertification and increased resource redistribution. *J. Geophys. Res.: Biogeosciences* 117. <https://doi.org/10.1029/2011JG001663>.

Fox, J., Weisberg, S., 2019. An R companion to applied regression, third ed. Sage, Thousand Oaks CA. URL: <https://socialsciences.mcmaster.ca/jfox/Books/Companion/>.

Grogan, P., Burns, T.D., Chapin III, F.S., 2000. Fire effects on ecosystem nitrogen cycling in a Californian bishop pine forest. *Oecologia* 122, 537–544. <https://doi.org/10.1007/s004420050977>.

Hoffmann, W.A., Geiger, E.L., Gotsch, S.G., Rossatto, D.R., Silva, L.C., Lau, O.L., Haridasan, M., Franco, A.C., 2012. Ecological thresholds at the savanna-forest boundary: how plant traits, resources and fire govern the distribution of tropical biomes. *Ecol. Lett.* 15, 759–768. <https://doi.org/10.1111/j.1461-0248.2012.01789.x>.

Högberg, P., 1997. 15N natural abundance in soil-plant systems. *Tansley Review No. 95. New Phytol.* 137, 179–203.

Jarvie, H.P., Jickells, T.D., Skeffington, R.A., Withers, P.J.A., 2012. Climate change and coupling of macronutrient cycles along the atmospheric, terrestrial, freshwater and estuarine continuum. *Sci. Total Environ.* 434, 252–258. <https://doi.org/10.1016/j.scitotenv.2012.07.051>.

Krishnamoorthy, K., Lee, M., 2014. Improved tests for the equality of normal coefficients of variation. *Comput. Stat.* 29, 215–232. <https://doi.org/10.1007/s00180-013-0445-2>.

Lajtha, K., Schlesinger, W.H., 1986. Plant response to variations in nitrogen availability in a desert shrubland community. *Biogeochemistry* 2, 29–37. <https://doi.org/10.1007/BF02186963>.

Levine, J.S., Winstead, E.L., Parsons, D.A., Scholes, M.C., Scholes, R.J., Cofer, W.R., Cahoon, D.R., Sebacher, D.I., 1996. Biogenic soil emissions of nitric oxide (NO) and nitrous oxide (N<sub>2</sub>O) from savannas in South Africa: the impact of wetting and burning. *J. Geophys. Res.: Atmosphere* 101, 23689–23697. <https://doi.org/10.1029/96JD01661>.

Li, J., Okin, G.S., Alvarez, L., Epstein, H., 2008. Effects of wind erosion on the spatial heterogeneity of soil nutrients in two desert grassland communities. *Biogeochemistry* 88, 73–88. <https://doi.org/10.1007/s10533-008-9195-6>.

McClaran, M.P., Moore-Kucera, J., Martens, D.A., van Haren, J., Marsh, S.E., 2008. Soil carbon and nitrogen in relation to shrub size and death in a semi-arid grassland. *Geoderma* 145, 60–68. <https://doi.org/10.1016/j.geoderma.2008.02.006>.

McCulley, R.L., Jobbagy, E.G., Pockman, W.T., Jackson, R.B., 2004. Nutrient uptake as a contributing explanation for deep rooting in arid and semi-arid ecosystems. *Oecologia* 141, 620–628. <https://doi.org/10.1007/s00442-004-1687-z>.

Peters, D.P., 2002. Plant species dominance at a grassland–shrubland ecotone: an individual-based gap dynamics model of herbaceous and woody species. *Ecol. Model.* 152, 5–32. [https://doi.org/10.1016/S0304-3800\(01\)00460-4](https://doi.org/10.1016/S0304-3800(01)00460-4).

Puttock, A., Macleod, C.J., Bol, R., Sessford, P., Dungait, J., Brazier, R.E., 2013. Changes in ecosystem structure, function and hydrological connectivity control water, soil and carbon losses in semi-arid grass to woody vegetation transitions. *Earth Surf. Process. Landforms* 38, 1602–1611. <https://doi.org/10.1002/esp.3455>.

Puttock, A., Dungait, J.A., Macleod, C.J., Bol, R., Brazier, R.E., 2014. Woody plant encroachment into grasslands leads to accelerated erosion of previously stable organic carbon from dryland soils. *J. Geophys. Res.: Biogeosciences* 119, 2345–2357. <https://doi.org/10.1002/2014JG002635>.

Qian, Y., Miao, S.L., Gu, B., Li, Y.C., 2009. Effects of burn temperature on ash nutrient forms and availability from cattail (*Typha domingensis*) and sawgrass (*Cladium jamaicense*) in the Florida Everglades. *J. Environ. Qual.* 38, 451–464. <https://doi.org/10.2134/jeq2008.0126>.

R Core Team, 2017. R: a language and environment for statistical computing. R Foundation for Statistical Computing, Vienna, Austria. URL: <http://www.R-project.org/>.

Rascher, K.G., Hellmann, C., Mágus, C., Werner, C., 2012. Community scale 15N isoscapes: tracing the spatial impact of an exotic N2-fixing invader. *Ecol. Lett.* 15, 484–491. <https://doi.org/10.1111/j.1461-0248.2012.01761.x>.

Ravi, S., D'Odorico, P., Wang, L., White, C.S., Okin, G.S., Macko, S.A., Collins, S.L., 2009. Post-fire resource redistribution in desert grasslands: a possible negative feedback on land degradation. *Ecosystems* 12, 434–444. <https://doi.org/10.1007/s10021-009-9233-9>.

Ravi, S., Baddock, M.C., Zobeck, T.M., Hartman, J., 2012. Field evidence for differences in post-fire aeolian transport related to vegetation type in semi-arid grasslands. *Aeolian Research* 7, 3–10. <https://doi.org/10.1016/j.aeolia.2011.12.002>.

Robinson, D., 2001. <sup>15</sup>N as an integrator of the nitrogen cycle. *Trends Ecol. Evol.* 16, 153–162. [https://doi.org/10.1016/S0169-5347\(00\)02098-X](https://doi.org/10.1016/S0169-5347(00)02098-X).

Sankey, J.B., Germino, M.J., Sankey, T.T., Hoover, A.N., 2012. Fire effects on the spatial patterning of soil properties in sagebrush steppe, USA: a meta-analysis. *Int. J. Wildland Fire* 21, 545–556. <https://doi.org/10.1071/WF11092>.

Schlesinger, W.H., Raikes, J.A., Hartley, A.E., Cross, A.F., 1996. On the spatial pattern of soil nutrients in desert ecosystems: ecological archives e077-002. *Ecology* 77, 364–374.

Throop, H.L., Archer, S.R., 2008. Shrub (*Prosopis velutina*) encroachment in a semidesert grassland: spatial–temporal changes in soil organic carbon and nitrogen pools. *Global Change Biol.* 14, 2420–2431. <https://doi.org/10.1111/j.1365-2486.2008.01650.x>.

Throop, H.L., Reichmann, L.G., Sala, O.E., Archer, S.R., 2012. Response of dominant grass and shrub species to water manipulation: an ecophysiological basis for shrub invasion in a Chihuahuan Desert grassland. *Oecologia* 169, 373–383. <https://doi.org/10.1007/s00442-011-2217-4>.

Throop, H.L., Lajtha, K., Kramer, M., 2013. Density fractionation and <sup>13</sup>C reveal changes in soil carbon following woody encroachment in a desert ecosystem. *Biogeochemistry* 112, 409–422. <https://doi.org/10.1007/s10533-012-9735-y>.

Van Auken, O.W., 2000. Shrub invasions of North American semiarid grasslands. *Annu. Rev. Ecol. Systemat.* 31, 197–215.

Van Auken, O.W., 2009. Causes and consequences of woody plant encroachment into western North American grasslands. *J. Environ. Manag.* 90, 2931–2942. <https://doi.org/10.1016/j.jenvman.2009.04.023>.

Wang, L., Okin, G.S., D'Odorico, P., Taylor, K.K., Macko, S.A., 2013. Ecosystem-scale spatial heterogeneity of stable isotopes of soil nitrogen in African savannas. *Landsc. Ecol.* 28, 685–698. <https://doi.org/10.1007/s10980-012-9776-6>.

Wang, G., Li, J., Ravi, S., Dukes, D., Gonzales, H.B., Sankey, J.B., 2018. Post-fire redistribution of soil carbon and nitrogen at a grassland–shrubland ecotone. *Ecosystems* 1–15. <https://doi.org/10.1007/s10021-018-0260-2>.

Wang, G., Li, J., Ravi, S., 2019. A combined grazing and fire management may reverse woody shrub encroachment in desert grasslands. *Landsc. Ecol.* <https://doi.org/10.1007/s10980-019-00873-0>.

White, C.S., 2011. Homogenization of the soil surface following fire in semiarid grasslands. *Rangel. Ecol. Manag.* 64, 414–418. <https://doi.org/10.2307/25835952>.

Zhou, Y., Mushinski, R.M., Hyodo, A., Wu, X.B., Boutton, T.W., 2018. Vegetation change alters soil profile <sup>15</sup>N values at the landscape scale. *Soil Biol. Biochem.* 119, 110–120. <https://doi.org/10.1016/j.soilbio.2018.01.012>.